NeuroImage 53 (2010) 1334–1345

Contents lists available at ScienceDirect

NeuroImage

journal homepage: www.elsevier.com/locate/ynimg

Distinguishing between lateralized and nonlateralized brain activity associated with visual short-term memory: fMRI, MEG, and EEG evidence from the same observers

Nicolas Robitaille [a,*], René Marois [b], Jay Todd [b], Stephan Grimault [a,c], Douglas Cheyne [d], Pierre Jolicœur [a]

[a] Centre de recherche en neuropsychologie et cognition, Département de psychologie, Université de Montréal, Montréal, Québec, Canada
[b] Vanderbilt Vision Research Center, Department of Psychology, Vanderbilt University, 530 Wilson Hall, Nashville, Tennessee 37203, USA
[c] Centre national de la recherche scientifique, France
[d] Program in Neurosciences and Mental Health, Hospital for Sick Children, Toronto, Ontario, Canada

ARTICLE INFO

Article history:
Received 5 May 2010
Revised 8 July 2010
Accepted 12 July 2010
Available online 16 July 2010

ABSTRACT

Previous functional neuroimaging studies have shown that maintenance of centrally presented objects in visual short-term memory (VSTM) leads to *bilateral* increases of BOLD activations in IPS/IOS cortex, while prior electrophysiological work suggests that maintaining stimuli encoded from a single hemifield leads to a sustained posterior *contralateral* negativity (SPCN) in electrophysiology and magnetoencephalography. These two findings have never been investigated using the same physiological measures. We recorded the BOLD response using fMRI, magnetoencephalography (MEG), and electrophysiology (EEG), while subjects encoded visual stimuli from a single hemifield of a balanced display. The EEG showed an SPCN. However, no SPCN-like activation was observed in the BOLD signals. The BOLD response in parietal cortex remained bilateral, even after unilateral encoding of the stimuli, but MEG showed both bilateral and contralateral activations, each likely reflecting a sub portion of the neuronal populations participating in the maintenance of information in VSTM. Contrary to the assumption that BOLD, EEG, and MEG responses – that were each linked to the maintenance of information in VSTM – are markers of the same neuronal processes, our findings suggest that each technique reveals a somewhat distinct but overlapping neural signature of the mechanisms supporting visual short-term memory.

© 2010 Elsevier Inc. All rights reserved.

Introduction

While behaving in a constantly changing environment, the visual system must maintain, in a readily available form, a portion of what was seen; a process supported by visual short-term memory (VSTM). Recently, important insights about the neural representation of VSTM were obtained following the identification of several new physiological markers of VSTM. Researchers have argued that the maintenance of information in VSTM is likely supported by the intra-parietal and intra-occipital cortex (IPS/IOS), because activity in these cerebral regions is strongly correlated with the amount of information held in memory (Todd and Marois, 2004). Conversely, lateralized visual stimuli, to be encoded and maintained for a brief period of time (e.g., 1 or 2 s), lead to sustained neural activity over the posterior regions of the cerebral cortex, contralateral to the stimuli to be encoded (Klaver et al., 1999). An increase of the amplitude of this memory-related ERP component (labeled SPCN, for Sustained Posterior Contralateral Negativity) as the number of items remembered increased was found (Brisson et al., 2008), and was subsequently used in several investigations of VSTM (Brisson and Jolicoeur, 2007; Jolicoeur et al., 2008; Robitaille and Jolicoeur, 2006; Robitaille et al., 2007).

These two physiological markers of VSTM (the BOLD response, and the SPCN) have several features in common. The topographical distribution of the SPCN (Brisson and Jolicoeur, 2007, 2008; Jolicoeur et al., 2008; McCollough et al., 2007; Perron et al., 2009; Robitaille and Jolicoeur, 2006; Robitaille et al., 2007) is very similar to that of the N2pc, for which parietal sources were identified(Hopf et al., 2000). The amplitudes of the electrophysiological and hemodynamic markers increase monotonically with the number of items presented, but reach a maximum at the subject's maximal VSTM capacity (e.g., calculated using Cowan's k formula (Cowan, 2001; Pashler, 1988)), creating a plateau for higher number of items. Moreover, both markers were linked to individual differences in VSTM capacity (Todd and Marois, 2005; Vogel and Machizawa, 2004). The most prominent difference between the SPCN and the BOLD activation in IPS/IOS is the encoding field manipulation used to isolate the SPCN. Indeed, the SPCN, as other ERP

Abbreviations: ER-SAM, event-related SAM; fMRI, functionnal magnetic resonnance imaging; IPS/IOS, intra-parietal/intra-occipital cortex; MEG, magnetoencephalography; MEM, maximum entropy of the mean; MNE, minimum-norm estimates; SAM, synthetic aperture magnetometry; SPCM, sustained posterior contralateral magnetic field; SPCN, sustained posterior contralateral negativity; VSTM, visual short-term memory.

* Corresponding author. BRAMS, Suite 0-120, Pavillon 1420 boul. Mont-Royal, Université de Montreal, C.P. 6128, Station Centre Ville, Montreal (QC), Canada H3C 3J7. Fax: +1 514 343 2175.
E-mail address: nicolas.robitaille@umontreal.ca (N. Robitaille).

1053-8119/$ – see front matter © 2010 Elsevier Inc. All rights reserved.
doi:10.1016/j.neuroimage.2010.07.027

components like the N2pc and the LRP, is based on a "contralateral–ipsilateral" difference to isolate the lateralized portion of the brain response, where the ipsilateral side of the brain is used as a control "condition," or as a control activation (Gratton, 1998) for the contralateral activation. This manipulation is intended to remove the effect of any activity that is not lateralized according to the stimulus presentation side (or response-button side, for LRP). Studies of VSTM using fMRI so far have used bilateral stimulus presentations and found bilateral activation in IPS/IOS.

The goal of the present study was to observe, directly, the relationship between the BOLD activation in IPS/IOS, the electrophysiological (SPCN) component, and the magnetoencephalographical (SPCM) marker of the maintenance of information in VSTM. We tested the same subjects both with fMRI and MEG – with EEG recorded simultaneously with MEG – in very similar experiments designed to allow comparisons across brain imaging modalities. To allow the use of a regression analysis on the number of items accurately held in memory (Todd and Marois, 2005), we presented 1, 2, 4, or 6 visual objects. We used bilateral stimulus presentations, with an arrow indicating which stimuli (on the left or right side of fixation) had to be encoded (Grimault et al., 2009; Robitaille et al., 2009; Vogel and Machizawa, 2004). This allowed us to compute both load-related activity (by collapsing trials with left-encoding and right-encoding) and an SPNC-like activation (using the "contralateral minus ipsilateral" measure) with the data from all imaging modalities. We recently coined the term SPCM, a magnetic equivalent of the SPCN (labeled SPCM for Sustained Posterior Contralateral Magnetic field) (Robitaille et al., 2009). Sensors showing the SPCM were located on two separate clusters of sensors, over parietal cortex. A critical finding of that study was that for different sensor clusters (different from the SPCM), we found an increase in magnetic field amplitude with the increase in the number of items held in memory that was independent from the encoding hemifield (i.e., no interaction between hemifield and the increase in activation as a function of memory load). This led us to conclude that a more complex network of neural generators was active during the retention period than what was isolated as the SPCM. However, this previous study only used two loads, preventing the use of a parametric analysis based on estimated memory capacity across loads (e.g., regression using Cowan's k (Todd and Marois, 2004)). Furthermore, anatomical MRIs were available for only 5 participants, which limited the possibility of source localization. These limitations were overcome here because an anatomical MRI was acquired for every subject and we used a broader range of memory loads.

The specific hypothesis we will test is that both physiological markers (BOLD activation in IPS/IOS and the SPCN/M) reflect the same underlying neural processes. In others words, the generators of the SPCN/M would be the left and right IPS/IOS; each of them would increase in activation level more for stimuli encoded from the contralateral side of space, relative to activation for stimuli encoded from the ipsilateral side. When stimuli are encoded from both sides of the screen simultaneously, the result would be a bilateral activation, as found in fMRI and suggested by the results of Klaver et al. (1999). We consider that this is commonly assumed, as both papers (Todd and Marois, 2004; Vogel and Machizawa, 2004) are often cited as though the SPCN/M and BOLD responses are different manifestations of the same underlying brain functions.

Methods

Subject

13 subjects were recorded in this experiment. One subject was excluded for a failure to maintain fixation during the task. The twelve remaining subjects (7 females) were between 19 and 31 years old (average 23.3), reported having no neurological problem and were able to easily discriminate the colors used in the memory task. For the first six subjects we counterbalanced the order of MEG and fMRI sequences. However, the three subjects who performed the fMRI first showed strong artifact in their MEG signal. To avoid further contamination of the MEG signal (of magnitude around 3e-14 Tesla) following the ~75 min exposure to the 3 Tesla magnetic field of the MRI, the remaining subjects did the MEG experiment first. An ICA artifact removal procedure (see below) successfully cleaned the MEG signals of the three subjects tested first with fMRI, so their results could be included in the analyses.

MEG and EEG

MEG and EEG procedures

Stimuli were presented on a back-projected translucent screen, located 75 cm in front of the subject. The area containing all the possible stimuli subtended 14° (width) by 7° (height) of visual angle centered within the display. Each trial started with the presentation, for 200 ms, of two arrowheads directly above and below the fixation point (see Fig. 1), with the arrowheads pointing to the left or the right of the screen. The fixation cross was then presented alone for 600 to 700 ms (varied randomly across trials). The random values were added so activity related to the arrows would not systematically overlap activity related to the memory array. On each side of the screen, 1, 2, 4, or 6 colored disks were presented for 200 ms (always an equal number on each side), at randomly selected positions within a 3×4 imaginary grid. Colors were selected among 8 highly discriminable colors (black, dark blue, green, light blue, pink, red, white, and yellow). A color was never repeated on one side of the screen, but selection was independent across sides. The retention period was 1000 to 1100 ms (randomly selected from a rectangular distribution), followed by the test display. The test display consisted of a colored disk (one on each side of the screen), located at the position of one disk presented for encoding. This display was presented for 1500 ms. On 50% of the trials, the test disk had the same color as the one previously presented at this location; otherwise it was of one of the 7 remaining colors. Subjects had 1500 ms to answer by pressing one of two keys on an optically-coupled response pad (right index for "same," right middle finger for "different"). A colored disk was always presented simultaneously on the other side of the screen, with color and position varied in the same way as for the test disk, but independently. Feedback was provided after each trial by changing the fixation cross to a + or − sign, for a correct or an incorrect answer, respectively. The feedback was presented for 600 to 900 ms, chosen on the basis of the previous random interval to create an average interval of 4400 ms (range: 4350 to 4450, selected from a rectangular distribution) between the onset of each trial. Trials were presented in 20 blocks of 40 trials. Subjects initiated the block manually, allowing for a rest period as needed. Trial order was counterbalanced.

The amount of information maintained in VSTM was assessed using Cowan's k formula (Cowan, 2001) based on the behavioral results: (proportion of hits − proportion of false alarms) * the number of items presented. This formula is useful because it corrects for possible biases in the propensity to respond 'same' or 'different' (see also Pashler, 1988).

MEG and EEG recordings

A CTF-VSM whole-head 275-sensor MEG system in a magnetically shielded room was used for the recordings. Data were filtered with a 150 Hz low-pass filter and digitalized at 600 Hz during the recording. Bad MEG channels (3 or 4, depending on the subject) were excluded from the recording. EEG (PO7, PO8, right mastoid) was also recorded with reference to the left mastoid, and later algebraically re-referenced to the average of the mastoids. Bipolar EOG (electrodes placed at the left and right canthi for horizontal EOG and above and below the left eye for vertical EOG) was recorded in order to monitor eye blinks and eye movements. Bipolar ECG was also recorded. Trials with a correct or an incorrect response were included in the brain signal analyses.

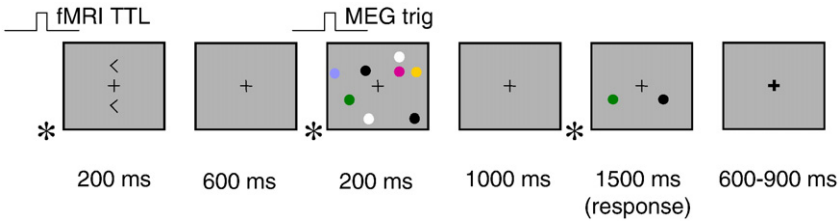

Fig. 1. Sequence of events in each trial. Stars refer to random intervals of 0–100 ms, which were compensated as needed after the response production to have a total duration of 4400 ms. A load 4, encode-left trial, requiring the answer "same" is illustrated, which received a positive feedback.

The ERP and MEG analyses were done using CTF software, EEGLAB (Delorme and Makeig, 2004), Fieldtrip, Brainvisa, Brainstorm, AFNI, and custom programs.

EEG analysis

The data were screened in order to remove trials containing eye blinks or eye movements, or artifacts in the electric signals. Trials were baseline-corrected based on the mean activity during the pre-encoding period (−200 to 0 ms, time relative to the onset of the memory array) and averaged. Amplitude of the SPCN was measured as the average voltage during the retention period (400 to 1200 ms). The SPCN was calculated as usual (amplitude for the contralateral sensor (PO7 for encode-right trials and PO8 for encode-left) minus amplitude for the ipsilateral sensor), for each load. A multiple regression was then performed for these values. The regression matrix contains a single predictor of interest (the behavioral k, centered), and dummy coding to remove the overall mean for each subject. The effect of load was also calculated by averaging the amplitude for both electrodes and stimulus location, for each load, and was submitted to the same type of regression.

MEG analysis

Trials with eye movements were removed because they could have been systematically correlated with the task (i.e., left movement for encode-left trials and right movement for encode-right trials). For each subject, we then performed an independent components analysis (ICA) of the entire data set. Components isolating activity from eye blinks, cardiac, or respiratory activity, were selected based on their topographies, their time-course, and their frequency signatures. Data were then back-transformed in signal-space (without these components), baseline-corrected (−200 to 0 ms) and averaged by conditions, producing event-related fields (ERFs). Statistical analyses were performed on the retention period on a sensor-by-sensor basis using the multiple linear regression analysis described earlier.

Beamformer analyses (ER-SAM) were performed using the raw data (prior to ICA), again with trials where subjects failed to keep fixation removed. This was deemed appropriate as beamformers can effectively reduce spatially stable noise, and data in which the artifacts were removed by ICA cannot be effectively used in the usual beamformer calculations due to a reduction of the rank of the data matrix. For each subject, a single weight matrix was calculated on the raw data of the entire experiment. Activation images were then produced for each conditions, averaged over the entire retention period. Use of a single weight matrix prevented any differences across conditions being attributed to differences in the weights with changing noise conditions. For ER-SAM, we used broadband activity (DC to 150 Hz) and the weights matrix was calculated from the onset of the memory array stimuli to the end of the retention period (0 to 1400 ms), after baseline correction (−200 to 0 ms). Images were calculated (spatial sampling resolution of 3 mm) at every time point of the retention period before being averaged.

Sources of the evoked magnetic fields were also estimated using cortically constrained weighted minimum norm (MNE; Brainstorm, and MEEG software tools from LENA-CNRS-UPR640, Cognitive Neuroscience and Cerebral imaging Laboratory) and Maximun of Entropy on the Mean (MEM (Amblard et al., 2004; Grova et al., 2006)). The cortical surface was extracted from the anatomical MRI scan using BrainVisa software. Approximately 8000 sources, oriented perpendicularly relative to the cortical surface, were distributed over the cortical surface, and these local sources were used in distributed source localization analyses. Event-related field for each condition, after being cleaned with ICA, were used as input for these analyses. MNE surfaces were computed with a Tikhonov parameter value of 10. MEM surfaces used activity during the baseline (−200 to 0) for a Multivariate source pre-localization (MSP). Images were computed for every time point in the retention period (400 to 1200 ms) before being averaged. Resulting images were interpolated back in the anatomical MRI space (voxels size: 4 mm3) of each subject, transformed in Talairach space using AFNI (Cox, 1996) and spatially smoothed (FWHM 12 mm). For ROI analysis, activation within a 7-mm radius sphere centered on the coordinate of interest was averaged in each map.

fMRI

fMRI procedure

The procedure was identical as for the MEG recordings except for two manipulations added to account for the overlap of the BOLD response across trials. First, random blank intervals were added between trials (52% without interval, 26% with one TR, 13% with two TRs, 6% with three, 3% with four), which allowed deconvolution analysis. Second, two blank conditions were added (arrow pointing to the left or right, but without stimuli or test afterward), for which time-course will also be extracted and subtracted from the time-course of experimental conditions. Each run consisted of 102 trials to allow counterbalancing of the order of the 10 trial types (2 sides × 4 loads, + 2 blanks), with a supplemental trial at the beginning and the end to ensure that all analyzed trials are preceded and followed by a trial of each possible type. Anatomical 3D high-resolution images were acquired using conventional parameters. Stimuli were back-projected on a translucent screen, visible via a mirror fixed onto the antenna. T2-weighted EPI images were acquired in AC–PC orientation, TR = 2200 ms, TE = 30 ms, FOV 24 cm, Flip Angle 70°, 28 axial slices of 64 × 64 voxels, 5 mm thick without slice gap, interleaved. Each subject performed 4 functional runs, followed by a high-resolution 3D anatomical scan. Data acquisition was performed with a 3 T Trio Siemens scanner at l'Unité de Neuroimagerie Fonctionnelle de l'Institut de Gériaterie de l'Université de Montréal. The first 8 subjects were tested with an 8-channel antenna on the Trio platform, the 4 last with a 12-channel antenna, on the Trio TIM platform after scanner upgrades.

fMRI analysis

Analyses were performed using AFNI (Cox, 1996) and in-house Matlab routines. Preprocessing consisted of slice-timing alignment, motion-correction, 8 mm FWHM spatial smoothing and within-run normalization. For each subject and condition, an SPM map was

created using multiple regression analysis, with regressors defined for each trial type and convolved with a canonical hemodynamic function (1 parameter gamma function (Cohen, 1997)). Influence of within-run trends (linear and higher-order) was removed by including regressors following Legendre polynomial trends (degree 5). This created 96 maps (12 subjects × 8 conditions), which were transformed into Talairach space before being submitted to a multiple regression analysis with regressors defined for k (balanced), for the Side factor, and for the interaction of k by Side, with a random-effect model. A false discovery rate (FDR) threshold of $q<.001$ was used to control for multiple comparisons in the Load maps, and of $q<.05$ for the Side map. We used a more liberal statistical threshold for the Side map because this is the first investigation of the effect of this manipulation in fMRI. Maxima were defined manually as the voxels with the highest activations in the corrected statistical maps. The time-course of the activation was extracted from a sphere (radius = 5 mm) centered on the maxima, using deconvolution. The activation time-course for the trials without stimuli to encode was subtracted from the time-course for experimental trials.

Results

Behavior

The number of items effectively encoded (calculated with Cowan's k formula (Cowan, 2001)) varied across set size and reached a plateau between 4 and 6 items, as shown in Fig. 2A, $F(3,33)=9.66$, $p<.0001$. All others factors (presentation side, first or second day of recording, fMRI or MEG recording) did not have a significant effect on k, all $Fs<1$. The group k values for each memory set size, averaged across both fMRI and MEG recording sessions (weighted by the number of trials in each), was used as the estimate of VSTM capacity at each load. These values were then used to create the load regressor, which will be used in the subsequent analyses of MEG, ERP, and fMRI data.

ERP — event-related potentials

The SPCN waveform amplitude increased during the retention period as load increased from 1 to 4, and then reached a plateau (Fig. 2C). The SPCN is calculated by subtracting the activation at the ipsilateral electrode (i.e., PO8 when the arrows pointed to the right and PO7 when the arrows pointed to the left) from the activation at the contralateral electrode (i.e., the contralateral minus ipsilateral difference). Note that the same type of calculation will be performed with all the physiological signals used in the study, namely we will compute an SPCM for the magnetic evoked field and an SPCN-like activation for the BOLD signal to quantify the degree to which the contralateral brain response is greater than the ipsilateral response. The amplitude of the SPCN during the retention period (400 to 1200 ms after the onset of the display), is plotted with SEM in Fig. 2B (green dashed curve), was significantly predicted by k, $F(1,35)=7.94$, $p<.008$. In order to compare to the fMRI analysis below, we also examined the overall effect of load in the average of the ipsilateral and contralateral ERP waveforms (rather than in the subtraction of these waves) (Fig. 2D). Robust initial visual components following the onset of the stimuli were present — this is because these waveforms are not subtraction waveforms. However, the amplitude of the ERP was not consistent through the retention period, and not significantly predicted by k, $F(1,35)=.034$, $p>.85$; see blue curve in Fig. 2D. The unsubtracted 'load' results probably reflect the contribution of multiple generators (e.g., sustained posterior negativity, on the one hand, and P3, on the other), and highlight the usefulness and importance of using the SPCN (contralateral minus ipsilateral difference waves) in the analysis of the EEG data, in the study of VSTM (Brisson and Jolicoeur, 2007; Mazza et al., 2007; McCollough et al., 2007; Robitaille and Jolicoeur, 2006; Vogel and Machizawa, 2004; Vogel et al., 2005).

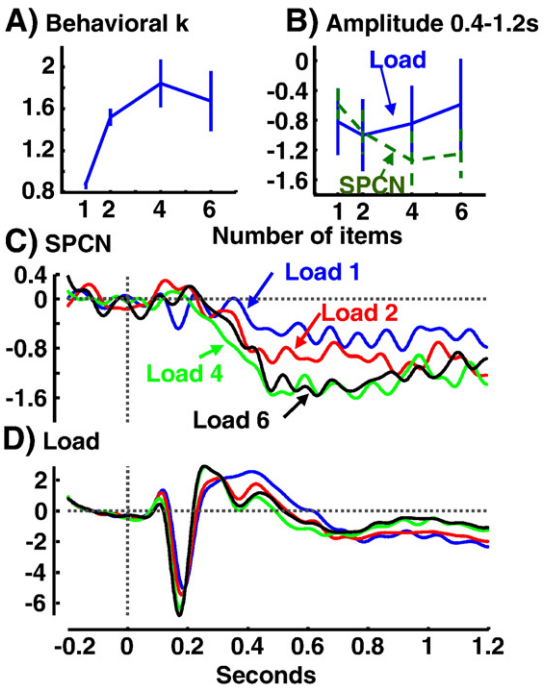

Fig. 2. (A) The number of items maintained in VSTM (k) increased from load 1 up to load 4 and then decreased slightly at load 6. The amplitude of the SPCN waveform (C) during the retention period, 400–1200 ms, followed k (green dashed line in B), but not the waveforms averaged for each load not taking side into account, shown in D (blue dashed line in B). SEM illustrated with vertical bars in A and B.

ERF — event-related fields

Load-sensitive channels (Fig. 3A) were identified with multiple regression of the MEG evoked fields. The two clusters of channels, each channel indicated with a bold dark circle, had a p-value inferior to .001 (uncorrected, channels evaluated independently). The left cluster contained 21 contiguous sensors with primarily ingoing (negative) fields during the sustained response and the right cluster of 20 contiguous sensors with primarily outgoing (positive) fields during the sustained response (the polarity of signals depends on the position and orientation of the neural generators relative to the sensors). The ERFs for the left cluster (Figs. 3B and C) showed evoked responses followed by sustained activity after the onset of the encoding-display. During the retention period, there was a clear differentiation of the waveforms according to the memory load conditions; the higher load showed higher amplitude from load 1 up to load 4, and no further increase from load 4 to load 6. The ERFs for the right cluster (Figs. 3E and F) showed again a clear differentiation as a function of memory load; higher load led to higher amplitude up to load 4 and a plateau across loads 4 to 6. For comparison between left and right sensors we inverted the polarity of left cluster channels. Combined activity of these waveforms during the retention period was significantly predicted by k, $F(1,35)=27.34$, $p<.0001$, (Fig. 3D). However, the SPCMs calculated from these waveforms were not significantly predicted by k, $F(1,35)=2.02$, $p>.16$.

Side-sensitive channels were also identified using multiple linear regressions (Fig. 3G). The posterior midline cluster contained 28 sensors. To avoid cancellation of the ERFs, we computed the average activity separately for the left and the right sensors within this cluster

(midline sensors were ignored). The 14 sensors in the left portion of the cluster had higher amplitude for the contralateral trials (Fig. 3H) than for the ipsilateral trials (Fig. 3I). Conversely, the 11 sensors in the right portion of the cluster showed higher activity for the contralateral trials (Fig. 3L) than for the ipsilateral trials (Fig. 3K). Combined activity (again here we transformed the left sensors to be negative-going) of these waveforms during the retention period (Fig. 3J, solid blue line) indicated a modulation by the load, for the overall load effect $F(1,35) = 15.56$, $p < .0001$. In order to determine if we could replicate here the SPCN effect, we also calculated the SPCM from these sensors (Fig. 3J, dashed green line). The amplitude of the SPCM across the load was significantly modulated by k, $F(1,35) = 12.31$, $p < .002$. This indicates that there are cerebrals regions (to be localized more precisely with the source localization analyses reported below) that emit a higher magnetic field when there is an increase in the number of items encoded from their contralateral hemifield.

Activity in the two anterior-most clusters was not significantly modulated by Load (both $Fs < 3.9$, $ps > .05$) or by the Load × Side interaction (both $Fs < 1.4$, $ps > .05$). Given that activity in these clusters was not affected by the memory load manipulation, we did not analyze them further.

These analyses of the ERFs indicated that the effects we were interested in were visible at the sensor level, and this justified the source localization analyses we present in subsequent sections of the article.

fMRI — functional magnetic resonance imaging

Results in Fig. 4 show load-related activity found using a regression on k on the fMRI BOLD. As expected from previous research we isolated a pair of symmetric posterior clusters containing the IPS/IOS coordinates (Todd and Marois, 2004). Within each cluster, three maxima were visible. For each bilateral pair of maxima (we

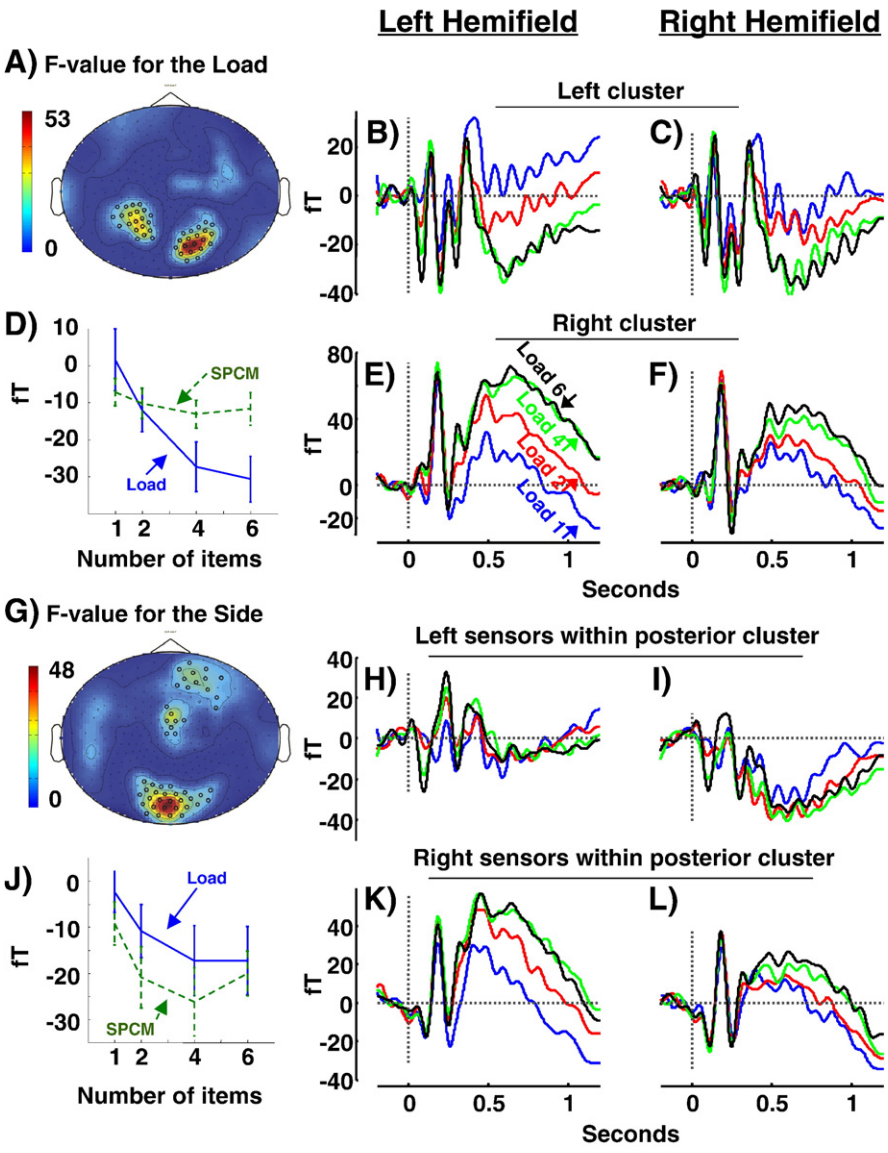

Fig. 3. The two posterior clusters of MEG sensors significantly modulated by k (A) showed robust activation throughout the retention period (B–C and E–F). The average waveforms for these sensors (with polarity adjusted) show an activation pattern during the retention period that was predicted by k (blue solid line in D), but they did not have a systematic modulation by side, which led to a flat amplitude across load for the SPCM (green dash line in D). The posterior cluster of MEG sensors significantly modulated by the side (G) was divided in a left (H–I) and a right (K–L) cluster. The averages waveform for these sensors (with polarity adjusted) show an activation during the retention period that was predicted by k (blue solid line in J), as did the SPCM calculated from these sensors (dashed green line in J).

defined maxima as a sphere of 5 mm surrounding the position of the voxel having the highest local activation), we extracted the time-course using deconvolution (see Fig. 5 for an example time-course). To examine more closely the effect of load, we averaged together the activity of the left and right maxima, for the encode-left and encode-right conditions (blue curves on the middle column of Fig. 4), at time 6.6 and 8.8 s. This activation was submitted to a multiple regression analysis, with k as the regressor of interest. This second analysis was intended as a direct test of the effect of mnemonic load for a specific pair of maxima located in homologous areas of the brain. It is indeed redundant in the present case (because these voxels were shown to follow k in the previous regression analysis), but it will allow a direct comparison of the effect of mnemonic load for different brain areas and most importantly for the SPCN-like BOLD signal described later in

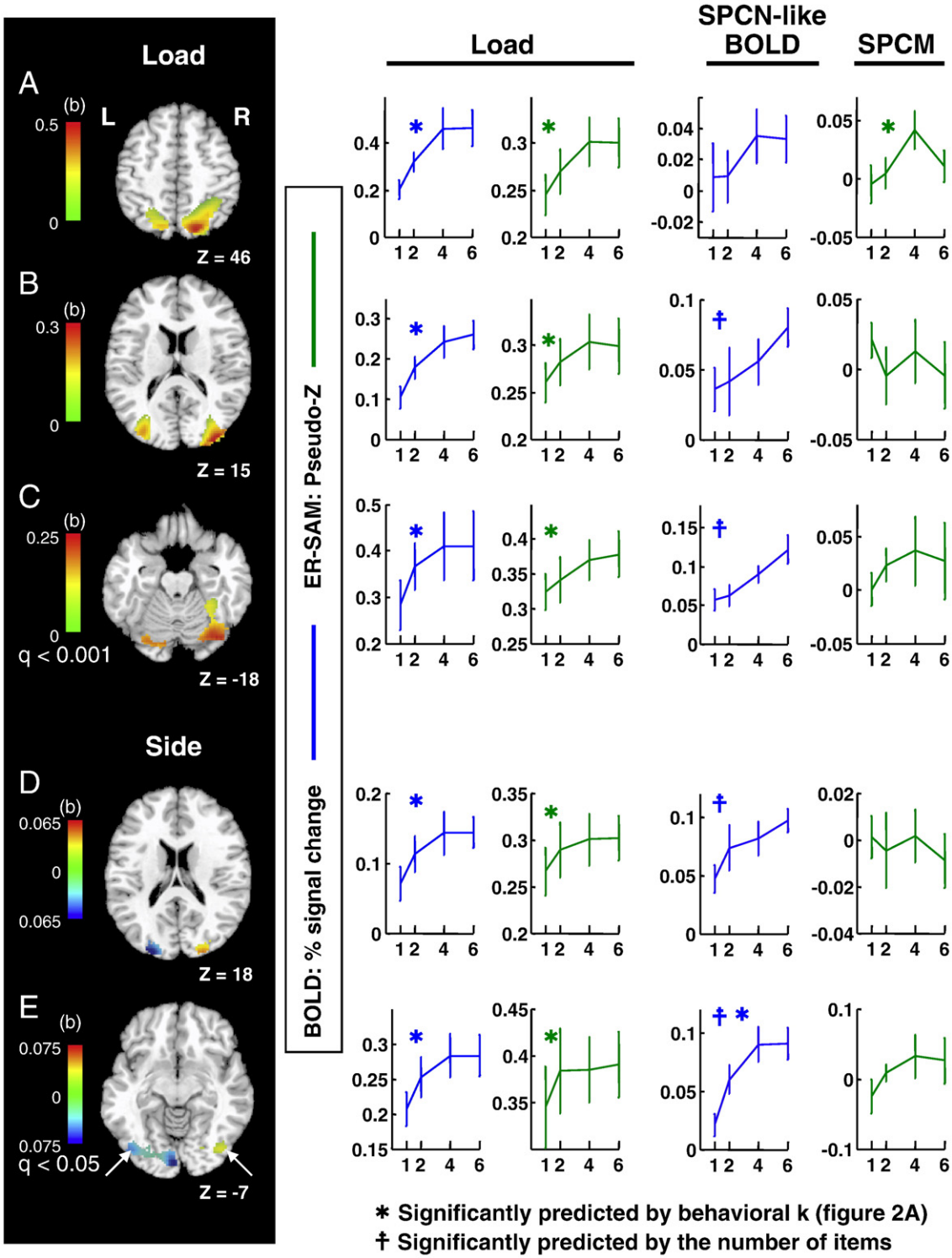

Fig. 4. Bilateral maxima found in the k-regression map in fMRI (first column) were the superior IPS (A), the IOS (B), and VO (C). The side map revealed the middle occipital cortex (D) and the inferior occipital (IO) cortex (E). The average amplitude of every maxima pair was predicted by k, either for the fMRI BOLD (blue curve) or the ER-SAM source analysis of the MEG signal (green curve). However, the SPCN-like activations calculated from these maxima were only significantly predicted by k for the ER-SAM in superior IPS (row A) or the fMRI BOLD in IO cortex (row E).

this paragraph. The number of items was also included as a covariate to remove any modulation of the response by the actual visual display. The superior IPS maxima (Fig. 4, row A) showed a clear modulation correlated with k, $F(1,34) = 5.11$, $p < .03$. The IOS maxima (Fig. 4, row B) were also significantly predicted by k, $F(1,34) = 12.01$, $p < .002$; as were the ventral–occipital (VO) maxima (Fig. 4, row C), $F(1,34) = 6.56$, $p < .02$. These results were expected because these maxima were identified on the load effect map. In order to compare these results with the EEG and MEG results, an SPCN-like BOLD activation was also calculated (blue curves of the third column of Fig. 4) by subtracting the activation of the ipsilateral maximum (left maximum for left stimuli and right maximum for the right stimuli) from the contralateral one. Although we found increases in BOLD signal strength that were larger on the contralateral side, none of them had a clear plateau between load 4 and load 6, and hence none was modulated by k, all $F(1,34) < 1$, all $p > .6$ (the number of items was also included as a covariate to remove any modulation of the response by the actual visual display). Overall, we found clear load effects that followed k when we averaged over left and right hemisphere maxima (replicating previous results (Todd and Marois, 2004)). However, we did not find an SPCN-like BOLD response that followed behavioral load effects, as estimated by k.

Superior IPS activation is shown in details for Fig. 5A. For both hemifield and maxima, the increase from load 1 to load 4, followed by a plateau for load 4 and 6 is visible. Furthermore, Fig. 5B recombines these data to create an ipsilateral (left maxima for stimuli on the left and right maxima for stimuli on the right) and a contralateral (right maxima for stimuli on the left and left maxima for stimuli on the right) time-course of activation. Either when the stimuli to be encoded are in the ipsilateral hemifield of the cerebral hemisphere we are recording, or in the contralateral hemifield, we observe the same pattern of activation. Thus, encoding visual stimuli from a single hemifield lead to a bilateral activation in superior IPS.

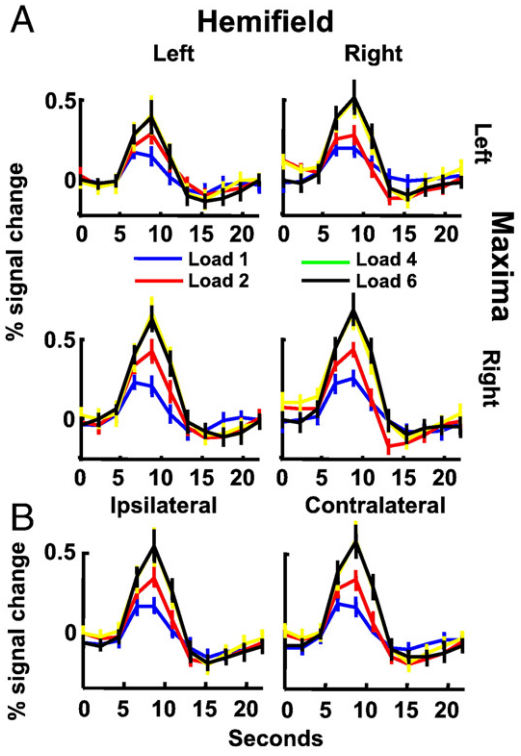

Fig. 5. Time-course of the BOLD activation in superior IPS. Left and right superior IPS showed the increase of activation for loads 1 to 4, and a plateau for loads 4 and 6. The similarity of the data in the ipsilateral and contralateral time-course (row B) indicates a bilateral activation.

We also determined which brain areas showed a BOLD response significantly different across the encode-left and encode-right conditions, independently of the number of items encoded. This "side map" (Figs. 4D and E) showed clusters of significant activation (corrected for multiple comparisons using False Discovery Rate: $q < .05$). The inversion of polarity across hemisphere indicates a systematic modulation according to the position of the stimulus to be encoded: activation was higher for stimuli encoded from the contralateral hemifield. We isolated three pairs of maxima in these maps. The first pair of maxima was located in the middle occipital gyrus, in Broadmann area 18; slightly more central and posterior than the IOS maxima (Fig. 4D; see Table 1 for the Talairach coordinates). Their activity was significantly predicted by k, $F(1,34) = 5.39$, $p < .03$. The activation in the second pair of maxima, located in the inferior occipital (IO) gyrus, was also significantly predicted by k, $F(1,34) = 8.84$, $p < .006$. Note that the arrows on Fig. 4E indicate these maxima. The medial activation in the left hemisphere did not have a homologous area to be compared with, so we did not include this region in the analysis. The third pair of maxima corresponded to the VO maxima described in the load maps. The SPNC-like BOLD activation, unlike what was found in any of the previously described maxima pairs, was significantly modulated by k for the IO maxima, $F(1,34) = 5.36$, $p < .03$. The time-course of the BOLD response, estimated by deconvolution for this pair of maxima, is shown in Fig. 6. For the left IO (top row of Fig. 6), the Load response was modulated by the position of the stimuli, leading to a significant Load × Side interaction, $F(1,80) = 11.92$, $p < .001$. The right IO BOLD Load response, on the contrary, was not influenced by the position of the stimuli, $F(1,80) = .19$, $p > .65$. The SPNC-like activation for the two others pairs of maxima (MOG and VO) was not modulated by Load, $F(1,34) < 1$.

The interaction (Load × Side) SPM map did not exhibit any significant activation, either using FDR or cluster threshold (Forman et al., 1995) when correcting for multiple comparisons. Thus, among the significant activations found in the fMRI data, the only candidate cerebral region for creating a load-related asymmetry similar to what is commonly found in EEG and MEG was the left IO.

An increase of activation for contralateral trials relative to ipsilateral trials, proportional to the number of items presented (rather than on the number of items encoded, as measured with k), was visible for several of the maxima pairs in parietal and occipital cortex. Multiple regressions indicated a significant correlation with the number of items for all the maxima pairs, all $Fs > 5.5$, all $ps < .025$, except for the superior IPS, $F(1,35) = 1.64$, $p > .20$. Consequently, there are three occipital maxima pairs, IOS, middle occipital, and VO, that did not show a correlation with k, but that showed one with the number of items presented for encoding. Given that the same number of items were presented in both attended and ignored hemifield; this effect is likely attributable to attention or memory-related factors. However, the absence of a plateau when the capacity of VSTM was exceeded indicates a processing step that is distinct from a pure working memory load effect and most likely corresponds to an attentional involvement in VSTM.

Table 1
Talairach coordinate of regions investigated.

	RH	LH
Superior IPS	16, −67, 49	−14, −69, 46
Inferior IPS (Xu and Chun, 2006)	26, −65, 34	−25, −70, 29
IOS	35, −85, 14	−31, −81, 15
Middle occipital	24, −86, 16	−21, −86, 18
IO (inferior occipital)	39, −72, −7	−40, −72, −7
VO	34, −69, −16	−26, −75, −15

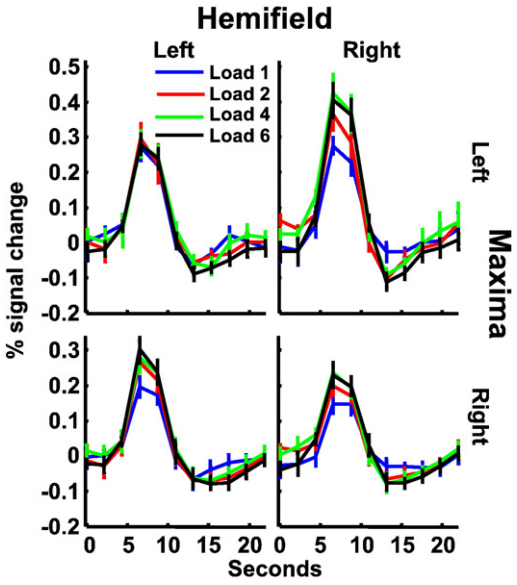

Fig. 6. Time-course of the BOLD activation in IO. Left IO showed a modulation of activation across load for contralateral trials (upper-left panel) but not for ipsilateral trials (upper-right panel). Right IO, however, showed a modulation for both ipsilateral and contralateral trials (lower panels).

ER-SAM–SPM on the source localization of the MEG signal

For each condition and subject, activation volumes were created using three source localization analyses (ER-SAM (Cheyne et al., 2006), MEM (Grova et al., 2006), and MNE (Hamalainen and Ilmoniemi, 1994)). The ER-SAM (event-related synthetic aperture magnetometry) analysis is a beamformer-based localization of the source of evoked field. Beamformer analyses use the covariance across the sensors in the raw data (i.e., trial-by-trial, before creating ERF) to maximize the activation at the estimated sources and minimize activation from others sources. The ER-SAM beamformer maximizes the signal time-locked to an event — here the apparition of the stimuli to encodes. The two other methods (MNE and MEM) take advantages of the anatomical information from each subject: an ensemble of pre-determined sources oriented perpendicular to the cortical surface (actually, the interface between the white and grey matter of the cortex) was used as the possible generator of the signal. The activation pattern of the sources leading to the recorded ERF is then estimated. This solution is constrained by minimizing the norm (MNE) or maximizing the entropy (MEM) of the solution. In the interest of space constraints, we show only the ER-SAM analysis here, but it should be noted that we found good agreement with MEM and MNE analyses. These methods are based on very different constraints and methods for source localization, and thus their convergence to the same sources is a good indication of their reliability (see Fig. 7, bottom row). The resulting 96 maps (12 subjects × 8 conditions) were then transformed in a normalized space (Talairach), and submitted to the same multiple linear regressions approach used for the fMRI data. To visualize the results, we overlaid them on a standard white-grey border surface, as shown in Fig. 7.

Significant load effects (False Discovery Rate: $q<.05$, top row of Fig. 7) consisted of three main cerebral activations. An increase of activation with load for the left and the right IPS/IOS cortex was visible, and was confirmed with MNE and MEM. The right frontal decrease of activation associated with the increase in mnemonic load included the right infero-frontal gyrus and the right claustrum. This decrease in amplitude, however, was not visible in MNE or MEM. The ER-SAM map showing the effect of side showed less extended activations. Similar to the fMRI results, there is an inversion of the activation values for the left and right posterior cortex, although this inversion occurred at different horizontal planes for the left and right hemispheres and was generally superior to the fMRI foci (see areas indicated by arrows in Fig. 7, bottom row). Although the MEM and MNE maps did not reach significance, lowering the threshold in these maps revealed the same regions. The interaction maps (Load by Side) did not reach significance in the sources localization analyses.

In order to compare the MEG activation with the results found for fMRI, we used the previously identified BOLD maxima as ROIs. We averaged the activation in the ER-SAM maps for a 7 mm radius sphere around the voxels of maximal BOLD activations (see Fig. 4, green curves). Statistical analyses were performed with multiple regression, and significance was assessed using permutation (Anderson and Legendre, 1999). Activation in all pairs of maxima was significantly predicted by k, all $ps<.009$. The same analysis conducted on the MEM and the MNE maps showed similar results. Thus, for every fMRI maximum found, the MEG activation showed an increase of activation as the number of stimuli increased, up to a plateau between 4 and 6. The SPCM was also calculated for these pairs of maxima. The SPCM for the superior parietal cortex was significantly predicted by k, $p<.022$. The IO gyrus (indicated by arrows in Fig. 4E) showed a marginal SPCM, $p<.07$; while all other SPCM calculations were not predicted by k, $ps>.11$. The SPCM on MNE and MEM maps did not reached significance, likely resulting from a lack of sensitivity of these methods. The parietal activations, thus, showed a higher response when the stimuli maintained in VSTM were encoded from their contralateral hemifield. This results contrast with the absence of SPCN-like activation in the BOLD signal for the same cerebral regions.

Literature-based inferior IPS ROI

Inferior IPS has been linked to processing of information in VSTM (Xu, 2007; Xu and Chun, 2006), but did not reveal itself in our maxima-based fMRI analysis. As we considered it important to describe the behavior of this region in our task, we defined ROIs base on Talairach coordinates from previous reports (see Table 1). They are located more lateral and inferior than our superior IPS, which is consistent with the anatomy of the IPS. The BOLD activation for this ROI is shown in Fig. 8. An increased of the BOLD activation as the number of items maintained in VSTM increased, thus showing a modulation by k, $F(1,34)=7.87$, $p<.009$, but the SPCN-like BOLD activation was not modulated by k, $F<.58$, $p>.44$. This pattern of results is identical to what was found for the superior IPS. The number of items, however, showed a significant correlation with the SPCN-like activation, $F(1,35)=5.23$, $p<.03$. Thus, the inferior IPS was the only cerebral region not in occipital cortex that showed a linear increase of activation for contralateral presentation of stimuli to be encoded. ER-SAM activation for these regions followed the same pattern: increase of activation with k, $p<.00001$, but the SPCN-like activation of ER-SAM activation was not predicted by k, $p>.21$. However, the SPCM pattern for the MNE activation in inferior IPS was significantly predicted by k, $p<.02$. Superior and inferior IPS are thus showing high concordance of activation, having a strong bilateral BOLD responses and magnetic evoked field increasing with the number of items held in VSTM. However, they also showed differences of activation for the SPCN-like BOLD response and SPCM activations, mainly a linear increase in contralateral BOLD responses that was present for inferior IPS only.

Discussion

We measured the memory-load-related activation patterns and the SPCN-like activation patterns for various physiological markers linked to VSTM derived from EEG, MEG, and fMRI brain imaging. The hemifield manipulation had limited impact on BOLD signal, whereas this manipulation was particularly useful to isolate the effect of

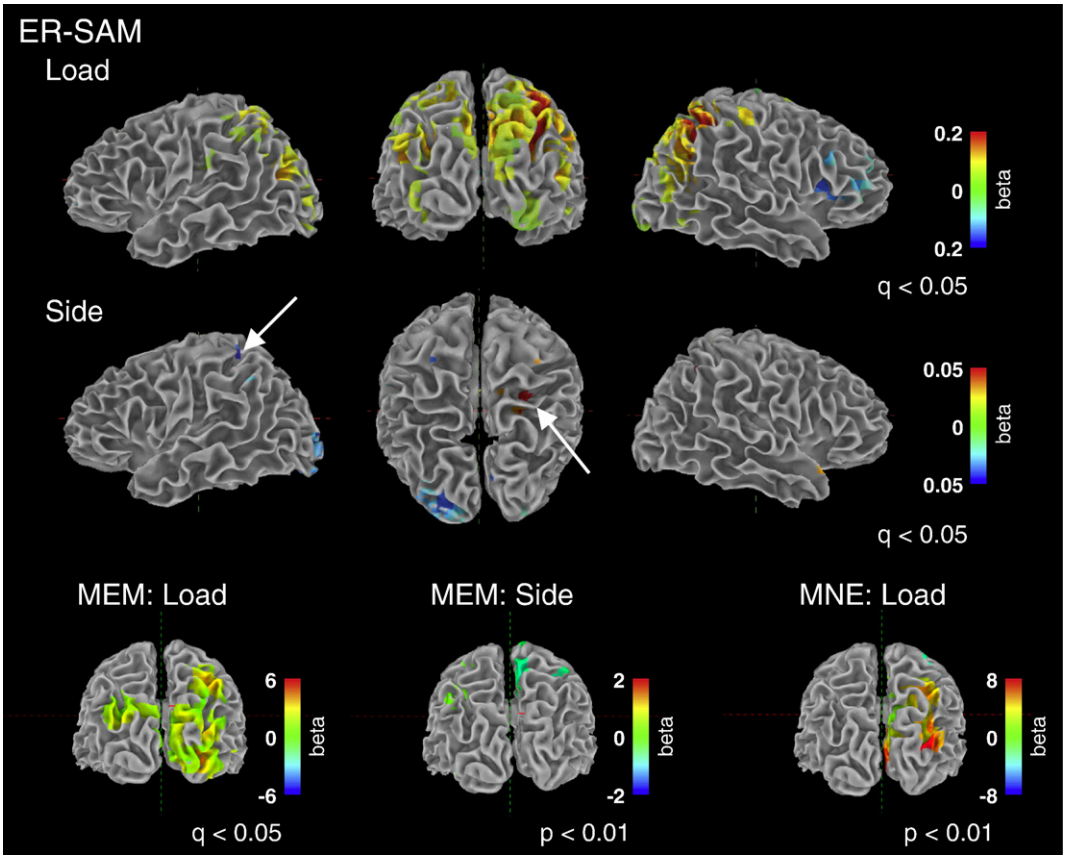

Fig. 7. Regression on k (top row) and on the stimulus presentation side (middle row) for the event-related beamformer source reconstruction, displayed on a template brain surface. The load activation was concentrated in the IPS/IOS area. Side-related activations (red for higher activation for encode-left trials and blue for higher activation for encore-right trials) were less extensive but visible for both left and right IPS (indicated with arrows) and in the left occipital cortex. Bottom row showed the maps for the MEM and MNE analysis. They converge with the ER-SAM analysis, but uncorrected threshold had to be used in the last two maps.

memory load in the ERPs. The evoked magnetic fields showed both a bilateral load-related increase and an SPCM effect.

Role of parieto-occipital areas in supporting VSTM

The superior IPS is likely one of the more important cerebral sources of the SPCM identified in the MEG sensor data, given that it

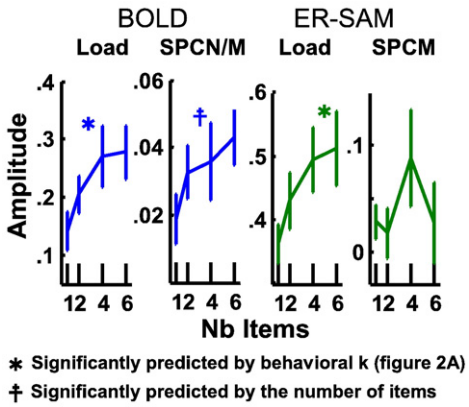

Fig. 8. Activations for the inferior IPS, as identified base on Xu and Chun's (2006) coordinates. A significant effect of load was found for the fMRI BOLD activation and the ER-SAM. The SPCN-like activation was not significant.

was the only cluster showing a significant increase of activation (as estimated with ER-SAM) with load, for contralateral stimuli. Superior IPS also showed an increase in BOLD signal for increasing memory load, consistent with previous study (Kawasaki et al., 2008; Song and Jiang, 2006; Todd and Marois, 2004, 2005; Xu, 2007; Xu and Chun, 2006). However, unlike what was expected, no SPNC-like activation pattern was found for the BOLD signal in IPS. That is, the increase in BOLD signal in the IPS was about the same in left and right IPS regardless of the side of visual space from which stimuli were encoded. This pattern of response is quite unlike what is found in the EEG and, to a lesser extent, the MEG results. It could be argued that we did not have the statistical power necessary to isolate such lateralized activity (although we did find significant lateralized activity, but this activity was linearly increasing with the number of items rather than limited by a plateau corresponding with VSTM capacity). However, the magnitude of the load-related manipulation was ten times higher than the magnitude of the (non-significant) SPCN-like BOLD activation, so even if the SPCN-like responses turned out to be statistically significant, the most predominant effect would still be a bilateral increase in activation. It is possible that the presence of ipsilateral stimuli reduced the lateralization of activity within IPS/IOS. Indeed, one may consider that ignored stimuli would also elicit a response, albeit smaller than for encoded stimuli. Using the same stimuli as for their VSTM experiment, two papers (Todd and Marois, 2004; Mitchell and Cusak, 2007) investigated the BOLD activation in IPS using an iconic memory task. Unfortunately, their results are not consistent: IPS showed a modulation of BOLD activation following k (as calculated for the VSTM task) in an iconic memory task for Cusack and Mitchell,

but not for Todd and Marois. Consequently, we cannot rule-out the possibility that the BOLD response in the ipsilateral IPS reflects the non-mnemonic activation found by Cusak and Mitchell instead of a bilateral encoding of the stimuli. If the absence of an SPCN-like response is caused by sensory activation of the ignored stimuli, this would, however, indicate that the BOLD response is sensitive to this sensory activation while the evoked magnetic field is not.

It is also possible that the mnemonic representation in IPS was initially unilateral, or more strongly lateralized, but progressively became more bilateral as the trial progressed. While EEG and MEG would have the temporal resolution to detect the initial difference and the reduction in the degree of contralateral dominance of the memory activity, it is possible that fMRI could not resolve this transient effect, with our scanning parameters. It is possible that the initial greater contralateral activity reflects, in part, a need to attenuate or suppress activity related to distractors presented in the visual field opposite to the one containing the target stimuli. This suppression would not have to be constant through the trial because the visual field is empty during the retention period. In support for this idea, the contralateral–ipsilateral difference waves tend to decrease in amplitude near the end of the trial, as visible, for example, in the results of Vogel and Machizawa (2004, Fig. 2) and here (Fig. 2C). Interestingly, there was no such reduction in a situation where distractors were present throughout the trials (Drew and Vogel, 2008). Although these changes are clearly visible in many EEG and MEG experiments, it is possible that the magnitude of these changes is sufficiently small and transient to make them more difficult to detect using standard fMRI methods. The present results do not contain strong evidence of a rapid reduction in the degree of contralateral dominance of the visual memory representation (e.g., Figs. 3B, C, E, and F), but the retention interval in the present study was relatively short. Additional research will required to test the present hypothesis.

The lack of agreement of the results for the superior IPS across MEG evoked fields and the BOLD signal is surprising given the strong agreement previously found between these two measures (Arthurs and Boniface, 2003; Arthurs et al., 2000; Dale et al., 2000; Logothetis et al., 2001). However, these studies used mainly the response of primary sensory areas, with transient and short-duration evoked fields (usually less than 100 ms) response to sensory stimuli, while here the evoked magnetic fields are of longer duration (1000 ms) and are related to higher cognitive functions. However, it was also shown that different modulations of the magnetic fields (DC shift, evoked-potential, and oscillatory activity for the alpha and gamma-band) show spatio-temporal covariance with the BOLD responses (Brookes et al., 2005). In the current paradigm, we previously showed a contralateral decrease and a bilateral increase of alpha-band oscillatory activity originating from parietal cortex in a very similar task (Grimault et al., 2009), and it is known that the displacement of spatial attention, as occurring here following the presentation of the arrowheads, does modulate parietal alpha-band oscillatory activity (Medendorp et al., 2007; Thut et al., 2006; Wyart and Tallon-Baudry, 2008). It is therefore possible that the SPCM observed here reflects the activity of a subpopulation of the neurons in superior IPS, but that the BOLD responses recorded from this region integrates the activity of more neurons, who do not all exhibit the same modulation of activation.

Inferior IPS showed a clear pattern here, the BOLD and ER-SAM overall load activations followed k, but neither had SPCN-like activation patterns. In a retention interval of 8300 ms, inferior IPS did not show a BOLD activation following the k-pattern, but rather a linear increase with the number of items (Experiment 3 of Xu and Chun, 2006). It was also found that sequentially presented stimuli at the center of the screen led to an equivalent BOLD response for loads 1 to 4, while sequentially presented stimuli at different eccentric locations led to an increase in activation with higher number of stimuli and therefore of spatial location, (Experiment 4 of Xu and Chun, 2006). Although these results suggested a dissociation between superior and inferior IPS based on the spatial content of the encoded information, the simple spatial manipulation used here (restricting encoding to one hemisphere) did not create differential memory-related activations between superior and inferior IPS. In addition, the IOS activations followed closely inferior IPS: increased mnemonic load led to an increase of the BOLD response, and of ER-SAM activations. Furthermore, a bilateral response to unilaterally-encoded stimuli was found for all of IPS/IOS cortex. Thus, our experimental manipulations did not reveal differences in BOLD activation patterns across the examined subportions of the IPS/IOS.

The ventral–occipital cortex activation isolated here was described earlier (Todd and Marois, 2004), but a specific role of this region for VSTM was discarded because this area, unlike the IPS/IOS cortex, showed an equivalent increase of activation with the behavioral k for an iconic memory task as for the VSTM task, and did not show a sustained activity with a longer 9200 ms retention interval. Furthermore, a linear increase of BOLD activation in VO following the increase of items presented to the subject (up to 8 items, well above VSTM capacity) was also found for an iconic memory task (Mitchell and Cusak, 2008). Although we did not perform such manipulations ourselves, their interpretation should apply to our situation, and thus we do not consider VO as paying a critical role in VSTM here. The middle occipital gyrus also showed a load-related activation pattern in our data, but only after being identified on the side SPM maps. ROI analyses are much more powerful than general SPMs – not being corrected for multiple comparisons – which could explain why it has not been identified previously. No SPCN-like activation was found for these maxima, however.

A linear increase of contralateral BOLD activation was found for occipital areas, as for the inferior IPS. Because this effect did not follow the behavioral memory pattern with a plateau following k, this likely does not reflect a process specific to VSTM. Our use of a balanced display, however, indicates that this effect is not related to the simple increase in the numbers of stimuli, but rather to an effect of attention.

Spatial attention vs. spatial location

Using fMRI, Sereno et al. (2001) identified a retinotopic map of spatial position encoded in short-term memory for IPS, a result that was further expanded to several maps along the IPS sulcus (Konen and Kastner, 2008). Like usual retinotopic maps, this one represents contralateral space, creating a significantly higher activation for contralateral than ipsilateral positions. Because our visual objects were created by the conjunction of a spatial location and a color, we were expecting to trigger a similar contralateral hemisphere bias in parietal activation to the one identified in Sereno and colleagues' work. Furthermore, the retinotopic organization found by Sereno and colleagues implies that different spatial positions are encoded by different groups of neurons, which should lead to a high summed activation when multiple locations are encoded. However, encoding several objects, each defined by the conjunction of a spatial location and a color, did not create asymmetries proportional to the number of items encoded (i.e., we did not find SPCN-like pattern in the BOLD response from IPS), but only a bilateral increase in BOLD activation. Some differences are evident across Sereno et al.'s design and ours. In their work, the target for which position was encoded was presented alone, thus possibly creating an initial stimulus-driven laterality. This would hardly be creating their effect because this retinotopic map was not identified with bright visual stimuli that did not require encoding in spatial short-term memory (Sereno et al., 1995). However, the presentation of the target alone could also create an exogenous shift of spatial attention (Posner and Cohen, 1984; Posner, 1980), which was not the case in the current study. The linear increase of contralateral BOLD activation that we found for inferior IPS (Fig. 8) suggested an effect of attention proportional to the number of items presented,

which could create the results found by Sereno and colleagues. Because they used a fixed mnemonic load (1 item), they could not distinguish between attention-related and memory-related activity using the plateau effect as we did here.

Another critical difference between their study and ours is the presence of a visual object to be encoded at each of the spatial locations to be encoded. Consequently, it is possible that the creation of an object-file by the binding of different features (spatial position and color were the only feature relevant to the task, but the stimuli also had a disk shape), which we know has strong impact on VSTM performance (Vogel et al., 2001), would also modify the neural pathway supporting the maintenance of spatial position, thus creating a different pattern of activation.

Inferior occipital cortex — unexpected activation

An SPCN-like pattern of activation was found in the BOLD response for the inferior occipital (IO) cortex isolated in the side fMRI activation map (Fig. 4E). The actual pattern of activation, however, was a modulation by load for the contralateral stimuli only in the left IO; the right IO had a load-related activation pattern for both encoding sides. The stimulation was equivalent for the left and right trials so this difference in activation can only be attributed to either spatial attention or to visual short-term memory. Spatial attention is known to modulate cerebral activation in the contralateral occipital cortex in absence (Kastner et al., 1999) or presence (Kastner et al., 1998) of visual stimuli. Shifting attention across visual field also creates contralateral activation in the occipital cortex (Kelley et al., 2007). Previous reports using a control task (Mitchell and Cusak, 2008; Todd and Marois, 2004) or a long retention period (Todd and Marois, 2004; Xu and Chun, 2006) did not investigate the specific involvement of IO in VSTM. Given that we were predicting, based on previous results, either a bilateral increase of activation or a contralateral increase of activation within each hemisphere for analogous cerebral regions, we do not have an empirically-supported interpretation for this activation (grounded in previous work). Further studies will be required to determine if the functional role of IO in lateralized VSTM task reflected mainly a spatial shift of visuospatial attention or if the mnemonic aspect of the task was crucial.

Strengths and limitations

A good concordance of source activation was visible across the different evoked field localization methods, with two main exceptions. First, the SPCN-like activation of the MNE for literature-based inferior IPS did follow k, which was not the case for the MEM or the ER-SAM. However, superior IPS did follow the SPCN-like pattern in ER-SAM, so this discrepancy is likely a difference in the precision of localization across methods. However, the right infero-frontal gyrus and the right claustrum decrease were only visible in ER-SAM, while other methods showed a non-significant increase of activation with the increase of mnemonic load at this location. For this reason, we do not wish to postulate a role for the right infero-frontal gyrus and the right claustrum in VSTM, although we consider worthwhile to report this result. Accordingly, despite the numerous advances in source localization of MEG signals, the use of multiple methods is still advised, along with careful interpretation of the results. The magnetic fields, however, were the only cerebral activity for which both bilateral and contralateral activations were found.

Conclusion

We studied several physiological markers of VSTM during maintenance of laterally-encoded stimuli. The BOLD activation in parietal cortex showed a bilateral increase in activation, independent of the location of the stimuli. This is in accordance with the magnetic fields, which also showed a bilateral increase in activation. These results converge with our previous work showing a bilateral increase of the ERF when the number of items was increased from 2 to 4 (Robitaille et al., 2009). This work, however, could not isolate VSTM process from other concurrent activations like attention because any difficulty-linked process would show a modulation of activation in these cases. Evoked field in MEG also showed a contralateral increase in activation for IPS, which likely represents the magnetic counterpart of the SPCN found in EEG.

References

Amblard, C., Lapalme, E., Lina, J.M., 2004. Biomagnetic source detection by maximum entropy and graphical models. IEEE Trans Biomed Eng 51, 427–442.

Anderson, M.J., Legendre, P., 1999. An empirical comparison of permutation methods for tests of partial regression coefficients in a linear model. Journal of Statistic and computer simulation 62, 271–303.

Arthurs, O.J., Boniface, S.J., 2003. What aspect of the fMRI BOLD signal best reflects the underlying electrophysiology in human somatosensory cortex? Clin Neurophysiol 114, 1203–1209.

Arthurs, O.J., Williams, E.J., Carpenter, T.A., Pickard, J.D., Boniface, S.J., 2000. Linear coupling between functional magnetic resonance imaging and evoked potential amplitude in human somatosensory cortex. Neuroscience 101, 803–806.

Brisson, B., Jolicoeur, P., 2007. A psychological refractory period in access to visual short-term memory and the deployment of visual–spatial attention: multitasking processing deficits revealed by event-related potentials. Psychophysiology 44, 323–333.

Brisson, B., Jolicoeur, P., 2008. Express Attentional Re-Engagement but Delayed Entry into Consciousness Following Invalid Spatial Cues in Visual Search. PLoS ONE 3, e3967.

Brisson, B., Leblanc, E., Jolicoeur, P., 2008. Contingent capture of visual–spatial attention depends on capacity-limited central mechanisms: evidence from human electrophysiology and the psychological refractory period. Biol Psychol.

Brookes, M.J., Gibson, A.M., Hall, S.D., Furlong, P.L., Barnes, G.R., Hillebrand, A., Singh, K. D., Holliday, I.E., Francis, S.T., Morris, P.G., 2005. GLM-beamformer method demonstrates stationary field, alpha ERD and gamma ERS co-localisation with fMRI BOLD response in visual cortex. Neuroimage 26, 302–308.

Cheyne, D., Bakhtazad, L., Gaetz, W., 2006. Spatiotemporal mapping of cortical activity accompanying voluntary movements using an event-related beamforming approach. Hum Brain Mapp 27, 213–229.

Cohen, M.S., 1997. Parametric analysis of fMRI data using linear systems methods. Neuroimage 6, 93–103.

Cowan, N., 2001. The magical number 4 in short-term memory: a reconsideration of mental storage capacity. Behavioral & Brain Sciences 24, 87–185 [References].

Cox, R.W., 1996. AFNI: software for analysis and visualization of functional magnetic resonance neuroimages. Comput Biomed Res 29, 162–173.

Dale, A.M., Liu, A.K., Fischl, B.R., Buckner, R.L., Belliveau, J.W., Lewine, J.D., Halgren, E., 2000. Dynamic statistical parametric mapping: combining fMRI and MEG for high-resolution imaging of cortical activity. Neuron 26, 55–67.

Delorme, A., Makeig, S., 2004. EEGLAB: an open source toolbox for analysis of single-trial EEG dynamics including independent component analysis. J Neurosci Methods 134, 9–21.

Drew, T., Vogel, E.K., 2008. Neural measures of individual differences in selecting and tracking multiple moving objects. J Neurosci 28, 4183–4191.

Forman, S.D., Cohen, J.D., Fitzgerald, M., Eddy, W.F., Mintun, M.A., Noll, D.C., 1995. Improved assessment of significant activation in functional magnetic resonance imaging (fMRI): use of a cluster-size threshold. Magn Reson Med 33, 636–647.

Gratton, G., 1998. The contralateral organization of visual memory: a theoretical concept and a research tool. Psychophysiology 35, 638–647.

Grimault, S., Robitaille, N., Grova, C., Lina, J.-M., Dubarry, A.-S., Jolicoeur, P., 2009. Oscillatory activity in parietal and dorsolateral prefrontal cortex during retention in visual short-term memory: additive effect of spatial attention and memory load. Hum Brain Mapp 30, 3378–3392.

Grova, C., Daunizeau, J., Lina, J.M., Benar, C.G., Benali, H., Gotman, J., 2006. Evaluation of EEG localization methods using realistic simulations of interictal spikes. Neuroimage 29, 734–753.

Hamalainen, M.S., Ilmoniemi, R.J., 1994. Interpreting magnetic fields of the brain: minimum norm estimates. Med Biol Eng Comput 32, 35–42.

Hopf, J.M., Luck, S., Girelli, M., Hagner, T., Mangun, G., Scheich, H., Heinze, H.J., 2000. Neural sources of focused attention in visual search. Cerebral Cortex 10, 1233–1241.

Jolicoeur, P., Brisson, B., Robitaille, N., 2008. Dissociation of the N2pc and sustained posterior contralateral negativity in a choice response task. Brain Res 1215, 160–172.

Kastner, S., De Weered, P., Desimone, R., Ungerleider, L.G., 1998. Mechanisms of directed attention in the human extrastriate cortex as revealed by functional MRI. Science 282, 108–111.

Kastner, S., Pisnk, M., De Weerd, P., Desimone, R., Ungerleider, L., 1999. Increased activity in human visual cortex during directed attention in the absence of visual stimulation. Neuron 22, 751–761.

Kawasaki, M., Watanabe, M., Okuda, J., Sakagami, M., Aihara, K., 2008. Human posterior parietal cortex maintains color, shape and motion in visual short-term memory. Brain Res 1213, 91–97.

Kelley, T., Serences, J., Giesbrecht, B., Yantis, S., 2007. Cortical mechanisms for shifting and holding visuospatial attention. Cerebral Cortex 18, 114–125.

Klaver, P., Talsma, D., Wijers, A.A., Heinze, H.-J., Mulder, G., 1999. An event-related brain potential correlate of visual short-term memory. Neuroreport: For Rapid Communication of Neuroscience Research 10, 2001–2005.
Konen, C.S., Kastner, S., 2008. Representation of eye movements and stimulus motion in topographically organized areas of human posterior parietal cortex. J Neurosci 28, 8361–8375.
Logothetis, N.K., Pauls, J., Augath, M., Trinath, T., Oeltermann, A., 2001. Neurophysiological investigation of the basis of the fMRI signal. Nature 412, 150–157.
Mazza, V., Turatto, M., Umilta, C., Eimer, M., 2007. Attentional selection and identification of visual objects are reflected by distinct electrophysiological responses. Exp Brain Res 181, 531–536.
McCollough, A.W., Machizawa, M.G., Vogel, E.K., 2007. Electrophysiological measures of maintaining representations in visual working memory. Cortex 43, 77–94.
Medendorp, W.P., Kramer, G.F.I., Jensen, O., Oostenveld, R., Schoffelen, J.-M., Fries, P., 2007. Oscillatory activity in human parietal and occipital cortex shows hemispheric lateralization and memory effects in a delayed double-step saccade task. Cerebral Cortex 17, 2364–2374.
Mitchell, D., Cusak, R., 2008. Flexible, capacity-limited activity of posterior parietal cortex in perceptual as well as visual short-term memory tasks. Cerebral Cortex 18 (8), 1788–1798.
Pashler, H., 1988. Familiarity and visual change detection. Perception & Psychophysics 44, 369–378.
Perron, R., Lefevbre, C., Robitaille, N., Brisson, B., Gosselin, F., Arguin, M., Jolicoeur, M., 2009. Attentional and anatomical considerations for the representation of simple stimuli in visual short-term memory: Evidence from human electrophysiology. Psychological Research 73 (2), 222–232.
Posner, M.I., 1980. Orienting of attention. Quarterly Journal of Experimental Psychology A 32, 3–25.
Posner, M.I., Cohen, Y., 1984. Components of visual orienting. In: Bouma, H., Bouwhuis, D. (Eds.), Attention and Performance, Vol. X. Erlbaum, pp. 531–556.
Robitaille, N., Jolicoeur, P., 2006. Fundamental properties of the N2pc as an index of spatial attention: effects of masking. Can J Exp Psychol 60, 101–111.
Robitaille, N., Jolicoeur, P., Dell'Acqua, R., Sessa, P., 2007. Short-term consolidation of visual patterns interferes with visuo-spatial attention: converging evidence from human electrophysiology. Brain Res 1185, 158–169.
Robitaille, N., Grimault, S., Jolicoeur, P., 2009. Bilateral parietal and contralateral responses during maintenance of unilaterally-encoded objects in visual short-term memory: evidence from magnetoencephalography. Psychophysiology 46, 1090–1099.
Sereno, M.I., Dale, A.M., Reppas, J.B., Kwong, K.K., Belliveau, J.W., Brady, T.J., Rosen, B.R., Tootell, R.B., 1995. Borders of multiple visual areas in humans revealed by functional magnetic resonance imaging. Science 268, 889–893.
Sereno, M.I., Pitzalis, S., Martinez, A., 2001. Mapping of contralateral space in retinotopic coordinates by a parietal cortical area in humans. Science 294, 1350–1354.
Song, J.-H., Jiang, Y., 2006. Visual working memory for simple and complex features: an fMRI study. Neuroimage 30, 963–972.
Thut, G., Nietzel, A., Brandt, S.A., Pascual-Leone, A., 2006. Alpha-band electroencephalographic activity over occipital cortex indexes visuospatial attention bias and predicts visual target detection. J Neurosci 26, 9494–9502.
Todd, J.J., Marois, R., 2004. Capacity limit of visual short-term memory in human posterior parietal cortex. Nature 428, 751–754.
Todd, J.J., Marois, R., 2005. Posterior parietal cortex activity predicts individual differences in visual short-term memory capacity. Cogn Affect Behav Neurosci 5, 144–155.
Vogel, Machizawa, 2004. Neural activity predicts individual differences in visual working memory capacity. Nature 428, 748–751.
Vogel, E.K., Woodman, G.F., Luck, S.J., 2001. Storage of features, conjunctions and objects in visual working memory. J Exp Psychol Hum Percept Perform 27, 92–114.
Vogel, E.K., McCollough, A.W., Machizawa, M.G., 2005. Neural measures reveal individual differences in controlling access to working memory. Nature 438, 500–503.
Wyart, V., Tallon-Baudry, C., 2008. Neural dissociation between visual awareness and spatial attention 2667–2679.
Xu, Y., 2007. The role of the superior intraparietal sulcus in supporting visual short-term memory for multifeature objects. J. Neurosci. 27, 11676–11686.
Xu, Y., Chun, M.M., 2006. Dissociable neural mechanisms supporting visual short-term memory for objects. Nature 440, 91–95.